

Photocatalytic degradation of organic pollutants using *Trianthema Portulacastrum* leaf extract based CeO₂ nanoparticles

A. Swetharanyam¹ & R. Kunjitham^{2*}

¹Research scholar, PG & Research department of chemistry, Department of Chemistry, Poompuhar College (Autonomous) Melaiyur - 609 107 (Affiliated to Bharathidasan University, Tiruchirappalli, Tamil Nadu- 620024); ²PG & Research department of chemistry, Department of Chemistry, Poompuhar College (Autonomous) Melaiyur - 609 107 (Affiliated to Bharathidasan University, Tiruchirappalli, Tamil Nadu- 620024), R. Kunjitham - Email: kunjithamr@gmail.com

Submitted on September 5, 2020; Revision September 9, 2020; Accepted September 11, 2020; Published October 31, 2020

DOI: 10.6026/97320630016765

The authors are responsible for the content of this article. The Editorial and the publisher has taken reasonable steps to check the content of the article with reference to publishing ethics with adequate peer reviews deposited at PUBLONS.

Declaration on official E-mail:

The corresponding author declares that official e-mail from their institution is not available for all authors

Declaration on Publication Ethics:

The authors state that they adhere with COPE guidelines on publishing ethics as described elsewhere at <https://publicationethics.org/>. The authors also undertake that they are not associated with any other third party (governmental or non-governmental agencies) linking with any form of unethical issues connecting to this publication. The authors also declare that they are not withholding any information that is misleading to the publisher in regard to this article.

Abstract:

Comparison of bio CeO₂-Nps prepared using *Trianthema Portulacastrum* leaf extract with chemical CeO₂-Nps is of interest. The ultraviolet - visible, x-ray diffraction, HR - TEM, FT - IR, and photoluminescence studies were conducted with CeO₂-Nps. UV-Maximum absorption at 292 nm was completed using UV-visible spectrum. The HR-TEM images showed 38 nm bio CeO₂-Nps with spherical morphology. This showed the polycrystalline character of CeO₂-Nps similar to XRD data. The presence of metal oxide is confirmed by FT - IR analyses. The CeO₂-Nps showed the potential photocatalytic activity for Acid black 1 color degradation after exposure to sunlight. Chem and bio CeO₂-Nps have a degradation rate of 86.66 and 94.33%, respectively for acid black 1 dye. The synthesized CeO₂-Nps are also evaluated for antibacterial and antioxidant activity. The bio CeO₂-Nps has antibacterial activity for *Pseudomonas aeruginosa* (17 ± 0.56 mm) and *Staphylococcus aureus* (16 ± 0.24 mm) at low concentrations of 100 µl. The CeO₂-Nps bio showed high inhibition of radical DPPH IC₅₀ 1 µg/ml, at 95.17 ± 21. Thus, we show that CeO₂-Nps have environmentally friendly properties that are useful for dye degradation with antimicrobial and antioxidant activities.

Keywords: CeO₂ nanoparticles, plant extract, dye degradation, antibacterial, antioxidant

Background:

The development of green chemistry to synthesize metal-based nanoparticles with extracts of different plants is gaining momentum in recent years [1]. Environmental impacts by bio nanoparticles are highly commended [2]. The plants have various types of phenolic and flavonoid compounds that help in nanoparticulate formation [3, 4]. It has been found that the extracts from various plants, such as *Cataranthus roseus* [6], *Cocos nucifera* [7], *Beta vulgaris* [8], *Catunareg amspinoso* [9] and *Cyphomandra betacea* were used to synthesize non-toxic nanomaterials [10]. The release of toxic substances affecting the environment by several industrial and research activities is evident [11]. Biosynthesized noble metal (Ag, Au... nanoparticles) are used for environmental friendly detoxification and elimination of harmful and deadly materials. [12, 13]. The mechanism of OH in biodegradation is known [14-16]. The formation π complexes as precursors of OH adduct in hydroxylated by-products with γ -radiolysis is described [17-19].

The NPs play an important role in the removal of organic and inorganic contaminants [20-22]. The bio CeO₂-NPs synthesis is environmentally friendly and non-toxic [23-24]. CeO₂-NPs are effective alternatives to degrade dyes and other pollutants [25-26]. Therefore, it is of interest to document the photocatalytic degradation of organic pollutants using bio (*Trianthema Portulacastrum* leaf extract) CeO₂ nanoparticles in comparison with the chemical CeO₂ nanoparticles.

Materials and methods:**Materials:**

Fresh *Trianthema portulacastrum* leaves were collected from chidambaram rural areas, Tamil Nadu, India. Cerium chloride (CeCl₃) (99.9%) was obtained and used as received by Sigma - Aldrich, Bangalore, India. *Staphylococcus aureus* (ATCC 6538) and *Pseudomonas aeruginosa* (ATCC 9022) were obtained from the microbial culture collection, the Institute of Microbial Technology in Chandigarh, India. Petri plates were selected with a diameter of about 32 cm and a thickness of 2 cm. All other used reagents are of analytical quality.

Preparation of CeO₂-Nps using chemical method:

Cerium chloride (CeCl₃) was used without further purification as they were received. CeO₂-Nps were developed using sol-gel processes [27]. 3.72 g cerium chloride salt taken in 10 ml of deionized water, and ammonia was added drop-by-drop until its pH attained 10. The continuous stirring for another two hours until all the precipitation was over. Filters wash and dry the precipitates overnight. The powder was then calcinated at a temperature of 400°C for two hours in an oven.

Preparation of CeO₂-Nps using plant extract method:

10g *Trianthema Portulacastrum* leaf was powdered and mixed with 100 mL of water at 80 °C. The extract of the leaf was filtered with Whatman No. 1. In 100-ml Erlenmeyer, it was preserved for further use at room temperature. 1:2 v/v CeO₂ were prepared using 10 ml CeCl₃ (contains 3.72g) and a 5 ml leaf extract. At a temperature of 85 °C, the mixture was agitated for 4 hours. The yielding of CeO₂-Nps observed yellowish-brown color. Also, the precipitate was dried for 4 hours at 400 °C.

Characterization of CeO₂-Nps

TEM images of metal oxide nanoparticles were obtained using a transmission electron microscope (PHILIPS CM200 model) at an operating voltage of 20-200kv with resolution: 2.4 Å. XRD spectra were recorded on the X'PERT PRO model X-ray diffractometer from Pan Analytical instruments operated at a voltage of 40 kV and a current of 30 mA with Cu K α radiation. The FT-IR spectra of powdered CeO₂ were mixed with KBr pellets and are recorded in the 4,000-400 cm⁻¹ range on a Shimadzu FTIR-8400s. To investigate optical responses and compute the bandgap, the synthesized CeO₂-NP samples have been subject to UV-vision spectroscopy (Shimadzu UV 1650). The energy for the nanoparticles optical band gap is calculated using the Tauc relation based on the absorption spectrum of the nanoparticles:

$$\hbar h\nu = A (h\nu - E_g)^{1/2}$$

Where \hbar is a coefficient of optical absorption, the photon energy is $h\nu$, E_g is a bandgap direct, and A is a constant that is energy-dependent.

Size of the synthesized CeO₂ Nps can be calculated by applying the following equation [28]:

$$D = 0.9\lambda / H \cos \theta \quad (\text{Scherrer equation})$$

If D is of crystalline size, k is of a shape factor ($K=0.9$ in this work), θ is of Bragg angle, H is of full width at half-maximum and λ is of wavelength of X-ray incident. Photoluminescence (PL) behavior was found at room temperature by FLUOROLOG-3.

Photocatalytic activity:

The photocatalytic activities of Chem CeO₂-Nps and plant mediated CeO₂-Nps were analyzed using the reactions of acid black 1 dye under-stimulated sunlight irradiation. In that experiment, 100 ml of 0.2 g of fine powder catalyst (Chem CeO₂-Nps and bio CeO₂-Nps) and 3×10^{-4} M aqueous acid black 1 dye were taken. Photocatalytic measurement time ranged between 0 and 80 minutes. The suspension allowed the adsorption to stir in

the dark for 10 min to achieve the adsorption-desorption balance between the dye and nanoparticles. Subsequently, the suspension was placed under sunlight and read every ten minutes up to 80 minutes.

On the catalyst surface, the proportion of acid black 1 was estimated following the following ratio [29]:

$$\text{Degradation (\%)} = C_0 - C_t / C_0 \times 100$$

where C_0 is the initial absorption and C_t is the absorption after different intervals of time.

Antioxidant studies using DPPH method:

1,1-diphenyl-2-picryl hydroxyl radical methods, as reported on Das *et al.* [30], have been tested in *Trianthema Portulastrum* leaf extract, Chem CeO₂-NP's, and Bio CeO₂-Nps. Added to 0.1 mM methanol DPPH radical solution in equal volume, the different concentrations of (25/50/100/125/250/500 µg/ml) sample solution were provided. The reaction mixture was incubated for 60 minutes at room temperature. The mixture has been measured for the optical intensity of 517 nm, which provides antioxidant activity. Ascorbic acid was used for the calibration of the resulting activity as standard. The radical scavenging activity (RSA) percentage of the sample was calculated using the following equation:

$$\% \text{ DPPH radical scavenging} = (\text{Absorbance of control} - \text{absorbance of test sample}) / (\text{Absorbance of control}) \times 100$$

Antibacterial activity:

Antibacterial properties of fresh leaf extract and prepared nanoparticles biological and chemical method has explored by using disc diffusion technic [31]. It has been studied using the clinical isolation of bacterial cultures Gram-positive bacteria and Gram-negative bacteria *Staphylococcus aureus* and *Pseudomonas aeruginosa* as well. Dissolved nutrient agar was swept into the bacterial suspension, poured through sterile swabs of cotton, and produced with the help of an adjustable cork borer made from stainless steel. At 35°C for 48 hours, the plates were incubated. Ciprofloxacin is used as a positive control and the 50 µl and 100 µl *Trianthema Portulastrum* leaf extracts, the Chem CeO₂-Nps and bioCeO₂-Nps were added. Table 3 shows the inhibition zone in diameter (mm).

Statistical analysis:

The results were evaluated statistically by sigma plot 12.5; an average value for three different replications and a standard error (SE) was determined.

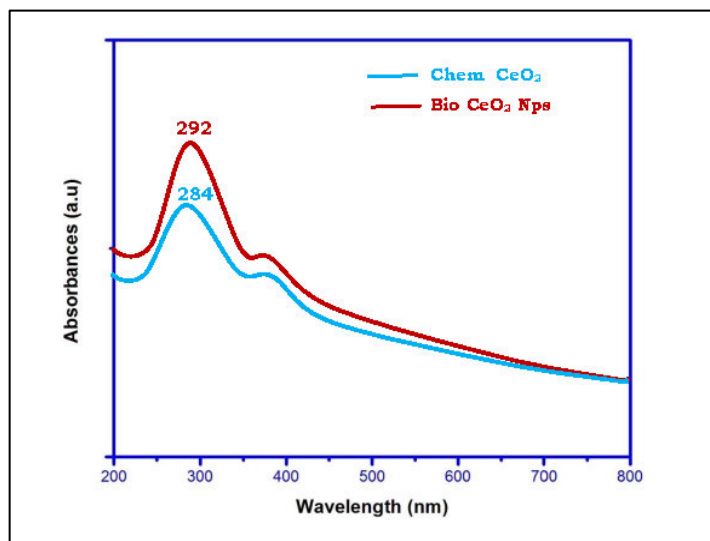


Figure 1: UV-visible spectra of Chem CeO₂-NPs and biosynthesized CeO₂-NPs

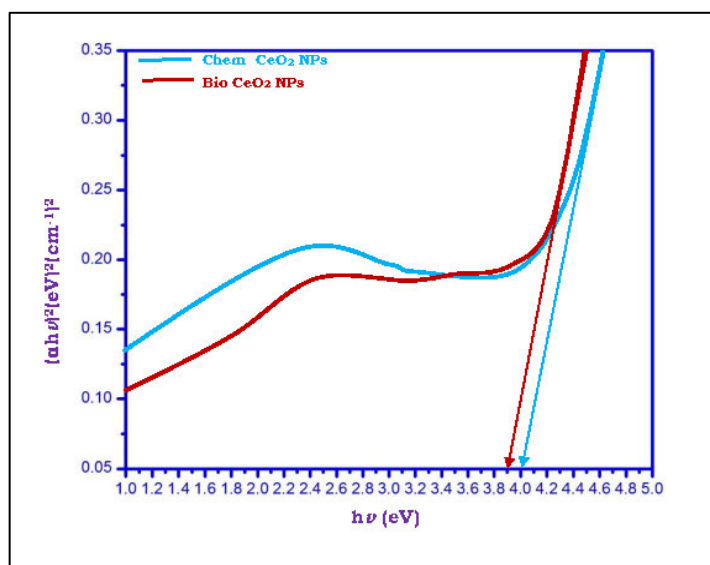


Figure 2: Band gap energy Chem CeO₂-NPs and biosynthesized CeO₂-NP

Results and Discussion:

Chemical CeO₂-Nps and bio CeO₂-Nps are measured using the optical absorption (Figure 1). Chem CeO₂-Nps and biosynthetic CeO₂-Nps at 284 and 292 nm absorption peaks are observed and all

these values are red shifts relative to the absorption maximum (284 nm) of the Chem CeO₂. Qaisar *et al* have shown similar absorption peaks (at 315 nm) for bio CeO₂-Nps [32]. The trianthema Portulastrum extract is comprised of phytochemicals that serve as a cap and reduction agent and also cause the UV absorption point to shift. The absorption position was suggested to depend on the size and shape of the particle in CeO₂-NP. The UV - visible absorption potential of the CeO₂-Nps is correlated with the bandgap energy, differentiating between CeO₂-Nps in different forms. Tauc's equation is used to compute the gap of synthesized CeO₂-Nps [33].

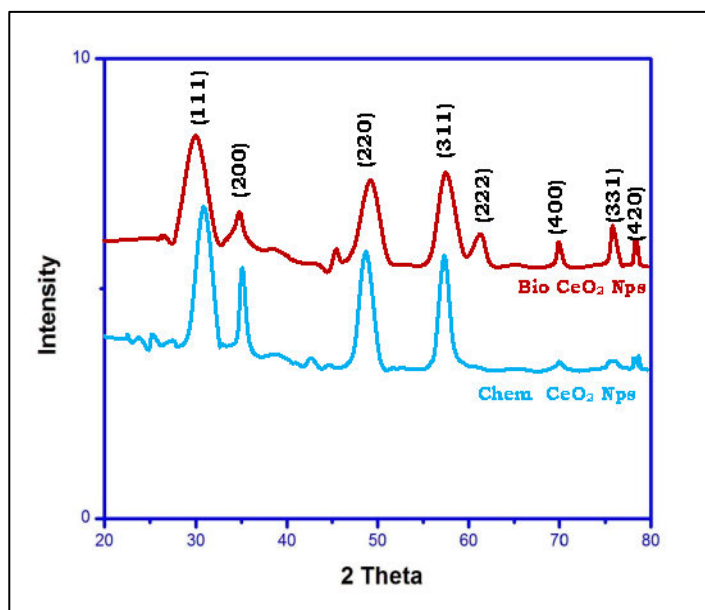


Figure 3: X-ray diffraction pattern of Chem CeO₂-NPs and biosynthesized CeO₂-NPs

Chem CeO₂-NP and bio CeO₂-NP band gap energy values have been identified 4.00 and 3.90 eV respectively (**Figure 2**). The band gap of the biologically synthesized CeO₂-Nps can be seen to be smaller than the Chem CeO₂-Nps. The powerful interaction between CeO₂ and *Trianthema portulastrum* leaf extract phytochemicals (flavonoids and proteins) allows for a faster process for recombining electrons and has resulted in a reduction in band gap for bio CeO₂ Nps. For CeO₂-NP-biosynthesized, the observed band gap value 3.90 eV is appropriate for photocatalytic and antibacterial activities, which involve electron-exciting formation.

Figure 3 shows the patterns of X-ray diffraction of chemicals CeO₂-Nps and bio CeO₂-Nps with various concentration of *Trianthema portulastrum* leaf extract. The sharp, intense diffraction peaks show Crystal structure and purity. The cubic structure of the CeO₂-Nps (Jcpds no: 043-2002) is the most responsive Bragg's Peaks that can be reported with the Miller Index (111), (200), [220], (400), (331) and [422] [34-35]. In determining the average crystallite sample size, the Scherrer formula has been used. **Figure 3** shows a crystal size of 78 nm for Chem CeO₂-Nps. With an increasing percentage of *Trianthema portulastrum* leaf extract; the crystal size decreases for bio CeO₂-Nps and is found to be 34 nm. Bio CeO₂-Nps are observed to have a minimum crystallite size due to their quantum confinement effect.

The FT - IR spectroscopy helps to detect leaf extract bio-molecules attached to the CeO₂ surface. FT - IR spectra for *Trianthema Portulastrum* dried leaf extract, Chem CeO₂-Nps and CeO₂-Nps bio are displayed in **Figure 4a-c**. **Figure 4a** shows the peaks and their assignments. FTIR spectroscopy illustrated absorption peaks at 3400, 2928, 1720, 1221 cm⁻¹ were reproduced in the extract of *Trianthema portulastrum* leaf. The absorption band of O-H stretching vibration appears at 3400 cm⁻¹. The absorption bands at 2928 and 1720 cm⁻¹ is due to aldehydic C-H stretching and C=O vibration, respectively. 1231 cm⁻¹ is due to C-N stretching vibration. Bio CeO₂-Nps shows FT - IR peaks at 3260, 2310, 1725, 1512, 1255, 1012 and 788 is due to presence of free O - H attachment [36-37], CH vibration, NH primary amines, CH₂ bond, CH₃ is due group, vinyl group and C -O stretching mode vibration [38]. The leaf extracts contain flavonoids that are potent reducing agents that can reduce cerium chloride heptahydrate salt. These flavonoids act as surfactants and are fixed to the CeO₂-NP surface, and by electrostatic stabilization, they stabilize CeO₂-NP's. As a result, *Trianthema portulastrum* leaf extract has a dual function to reduce and stabilize CeO₂-Nps.

Photoluminescence spectroscopy (PL) usually explores the efficiency of the migration and transmission of charging carriers and also the chance of electron-hole pairs in metal oxide [39]. In this research, Photoluminescence spectrum is used to collect significant evidence about surface defects, oxygen vacancies and surface conditions which may sulphurise the impact of the photocatalytic response. The Chem CeO₂-Nps and bio CeO₂-Nps show room temperature PL spectrum in Fig 5. The two samples show similar peak positions but vary in intensity. With increasing leaf extract *Trianthema portulastrum* percentage the PL intensity increases. The synthesized CeO₂-NP emission spectrum includes three peaks of 385, 443 and 469 nm, which reflecting the near-band emissions one violet and two blue emissions. Excitonic recombination is the result

of the Chem CeO₂-Nps PL emittance peak at 389 nm. It is due to the transitions of 5d-4f of Ce³⁺ from ground state 2D(5d1) to state 2F_{5/2}(4f1) [40]. At 443 and 469 nm, the emission peak is related to oxygen vacancies [41-42]. The bio CeO₂-Nps has a blue - shift at 443 nm and 469 nm compared with the chem CeO₂-Nps. The blue emission peak lies at 443 nm due to the transition from the oxygen vacancy. The oxygen defects in bio CeO₂-Nps thus support to connect the photo - induced electron easily in excitons. This shows that the intensity of PL has increased. The enhanced PL shows the intensity of bio CeO₂-Nps ' good crystalline nature and shows desirable catalytic properties.

The morphological and particulate sizes of the synthesized CeO₂-Nps are demonstrated by high - resolution transmission electron microscopy (HR-TEM). The figures 6a & 7a show typical TEMs obtained with CeO₂-Nps prepared using trianthema Portulacastrum extract and Chem CeO₂-Nps. Synthesized CeO₂-Nps have a morphology of almost cubic nanocrystals. In Figures 6d & 7d the histogram showing the distribution of particle size. The histogram in the bioCeO₂-Nps and chemicals CeO₂-Nps is narrower in width and the mean particle size is 38 and 82 nm. The particle size seen in HR-TEM is less than the dynamic light scattering value. The electron (SAED) pattern selected for the area is confirmed with the crystal plane nature of a bio CeO₂-Nps, with the bright-circulated spots that correspond to the following (1 1 1), (2 2 0) (2 2 1), (2 2 2), (4 0 0), (3 3 1) and (4 2 0). The SAED pattern of crystalline impurities shows no other rings [43-44].

Photocatalytic activity:

CeO₂-Nps are environmentally friendly among many rare earth elements, due to their ecologically based photocatalytic application. Industrial waste contains various types of toxic and organic dyes released into water bodies. It has a major environmental impact. All dyeing agents are organically stable. The colors of acid black 1 dye in both oxidized and reduced shapes are different, so it is picked for the study.

For chemical CeO₂-Nps and bio CeO₂-NP, photocatalytic activity is conducted to investigate the degradation of an aqueous acid black 1 dye solution by open-air sunlight. In Figure 8a-d you can see the catalytic degradation of the dye. The spectrum UV -Vis is recorded at different intervals 0, 20, 40, 60 and 80 min, between 200 and 800 nm. If it is acid black 1 dye, the peak UV absorption at 345 and 615 nm indicates that the dark blue of the dye becomes a colorless due to electron transition. The bands of 615 nm show that, owing to the catalytic effectiveness Chem CeO₂-NP and the bio CeO₂-N Ps, 86.66 and 94.33% of dye are exactamente 80 minutes degraded (Table 1). When the catalyst is added, the increased reduction rate is

observed. This refers to the potential redox enhancement of the electron movement process between beneficiary and recipient. Bio CeO₂-Nps act as an effective redox catalyst with an electron relay effect. The size of metal nanoparticles plays a major role in catalytic reductions, while the size of bio CeO₂-Nps has decreased that promotes reactant adsorption on the catalyst surface and simplifies degradation. This will greatly improve the efficiency of the catalyst by increasing the particle surface area. Table 2 shows reusability efficiency of bio and chem CeO₂, upto two cycles there is no decrease in percentage degradation of acid black 1 dye

Mechanistic pathway of dye degradation:

The various quantities of oxygen vacancies show that photocatalytic results are different. It further suggests that significantly more oxygen vacancies will require quick recombination of electron holes and thus decrease photocatalysis for Chemical CO₂-Nps [45]. The difference in photocatalytic activity has highly been linked in accordance with concentration errors on the nanoparticles surface [45]. They also showed that surface defects have been increased as the particle sizes decreased and photocatalytic activity increased. The present study shows high photocatalytic activity in bio-synthesized CeO₂-Nps with the smallest particle size attributable to the high separation capacity of the photo generating chargers, large specific areas, and increased absorption of light. Based on these, the possible photo-degradation of the Acid black 1 dye over the UV-radiated CeO₂-Nps is shown in Figure 8.

The above reaction stages allow electrons (e⁻) to be excited into the conductivity band (CB) by sunlight when the bi-synthesized CeO₂-NP is radiated by the same number of holes (h⁺) in the VB. Photo-initiated holes react reasonably with Acid black 1 or attach to the surface H₂O or OH \square bound to provide a solid oxidant OH \square radical species. It is suggested that the produced electron binds to O₂ adsorbed to produce O₂⁻. This means that H⁺ produces HO₂[·], which leads to radical OH[·] from the trapped electron. Therefore, the Acid black 1 dye could be degraded by produced reactive species such as OH[·], HO₂[·], and O₂⁻.

Kinetic studies:

The kinetics of photocatalyst organic degradation in pseudo-first order is described elsewhere [46].

$$\ln(C_0/C_t) = -kt$$

Where k is the apparent reaction rate constant, C₀ is an initial concentration of aqueous Trypan blue, t is a time of reaction and C

is an aqueous Acid black 1 color at a time of reaction t . Bio-synthesized CeO₂-Nps and Chem CeO₂-Nps are investigated and the kinetics of photodegradation of Acid black 1 is presented in **Figure 8a, b**. A pseudo-first-order rate equation determines the rate constant (K) for Acid black 1 dye degradation using synthesized CeO₂-Nps. The graph $\ln(C_0 / C_t)$ is a rate constant of bio and chemically synthesized CeO₂ Nps 7.8524 and 5.5924 min⁻¹ based on the irradiation duration. Also, 0.9832 and 0.9750 for Chem CeO₂-Nps and CeO₂-Nps bio are also determined for the fitting

correlation coefficient (R^2). Finally, C_0/C_t decreased with time increasing and vice versa. With the increase in time, the percentage of degradation is increased (**Figure 8d**). As a result, BioCeO₂-Nps demonstrated an improved photocatalytic efficiency in Acid black 1 dye than Chem CeO₂-Nps and other literature values.

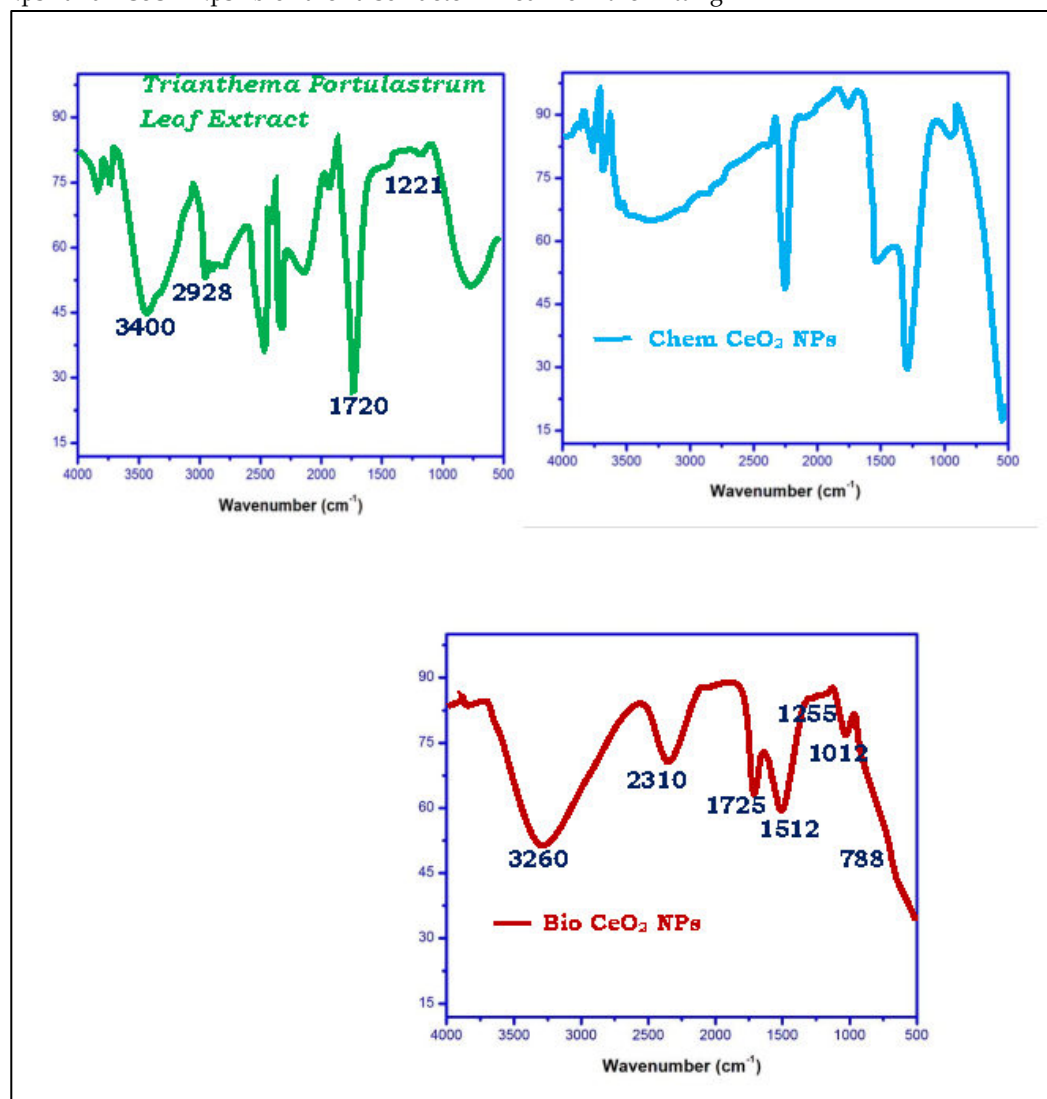


Figure 4: FT-IR spectrum of *Trianthema portulastrum* leaf extract, Chem CeO₂-NPs and biosynthesized CeO₂-NPs

Table 1: % degradation of acid black 1 dye compared to the Chem CeO₂-NPs and biosynthesized CeO₂-NPs

| Time (min) | % Degradation of acid black 1 dye | |
|------------|-----------------------------------|---------------------------|
| | Bio CeO ₂ NPs | Chem CeO ₂ NPs |
| 0 | 0 | 0 |
| 20 | 32.14 | 28.41 |
| 40 | 46.58 | 39.28 |
| 60 | 63.65 | 54.57 |
| 80 | 75.1 | 68.74 |
| 100 | 94.33 | 86.66 |

Table 2: Reusability of acid black 1 dye compared to the Chem CeO₂-NPs and biosynthesized CeO₂-NPs

| Cycles | 1 | 2 | 3 | 4 | 5 |
|-----------------------|----|----|----|----|----|
| Bio CeO ₂ | 94 | 94 | 92 | 92 | 88 |
| Chem CeO ₂ | 86 | 86 | 84 | 82 | 80 |

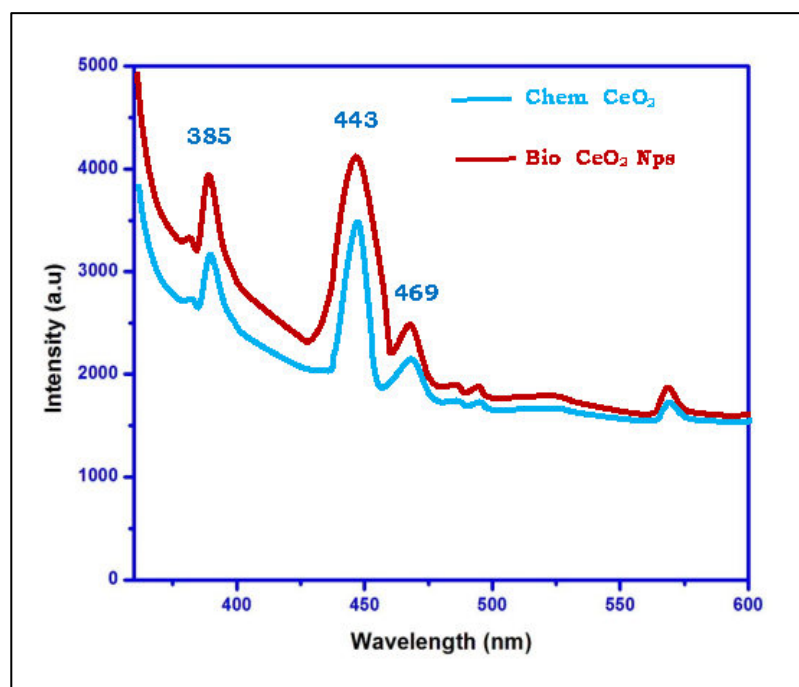


Figure 5: Photoluminescence spectra of Chem CeO₂-NPs and biosynthesized CeO₂-NPs

Table 3: DPPH free radical assay of Trianthema Portulastrum leaf extract, ChemCeO₂-NPs and biosynthesized CeO₂-NPs

| Compound | Concentration $\mu\text{g/ml}$ | | | | | | IC ₅₀ |
|---------------------------|--------------------------------|---------------|---------------|---------------|---------------|---------------|------------------|
| | 25 | 50 | 100 | 125 | 250 | 500 | |
| Leaf extract | 12 \pm 0.23 | 21 \pm 0.54 | 35 \pm 0.07 | 48 \pm 0.28 | 57 \pm 0.25 | 69 \pm 0.25 | 102.52 |
| Chem CeO ₂ NPs | 21 \pm 0.12 | 32 \pm 0.87 | 460.13 | 57 \pm 0.45 | 65 \pm 0.14 | 80 \pm 0.58 | 104.86 |
| Bio CeO ₂ NPs | 28 \pm 0.09 | 39 \pm 0.65 | 51 \pm 0.45 | 68 \pm 0.57 | 76 \pm 0.36 | 89 \pm 0.47 | 95.17 |
| Standard | 32 \pm 0.45 | 46 \pm 0.35 | 59 \pm 0.23 | 74 \pm 0.31 | 84 \pm 0.69 | 96 \pm 0.98 | 88.49 |

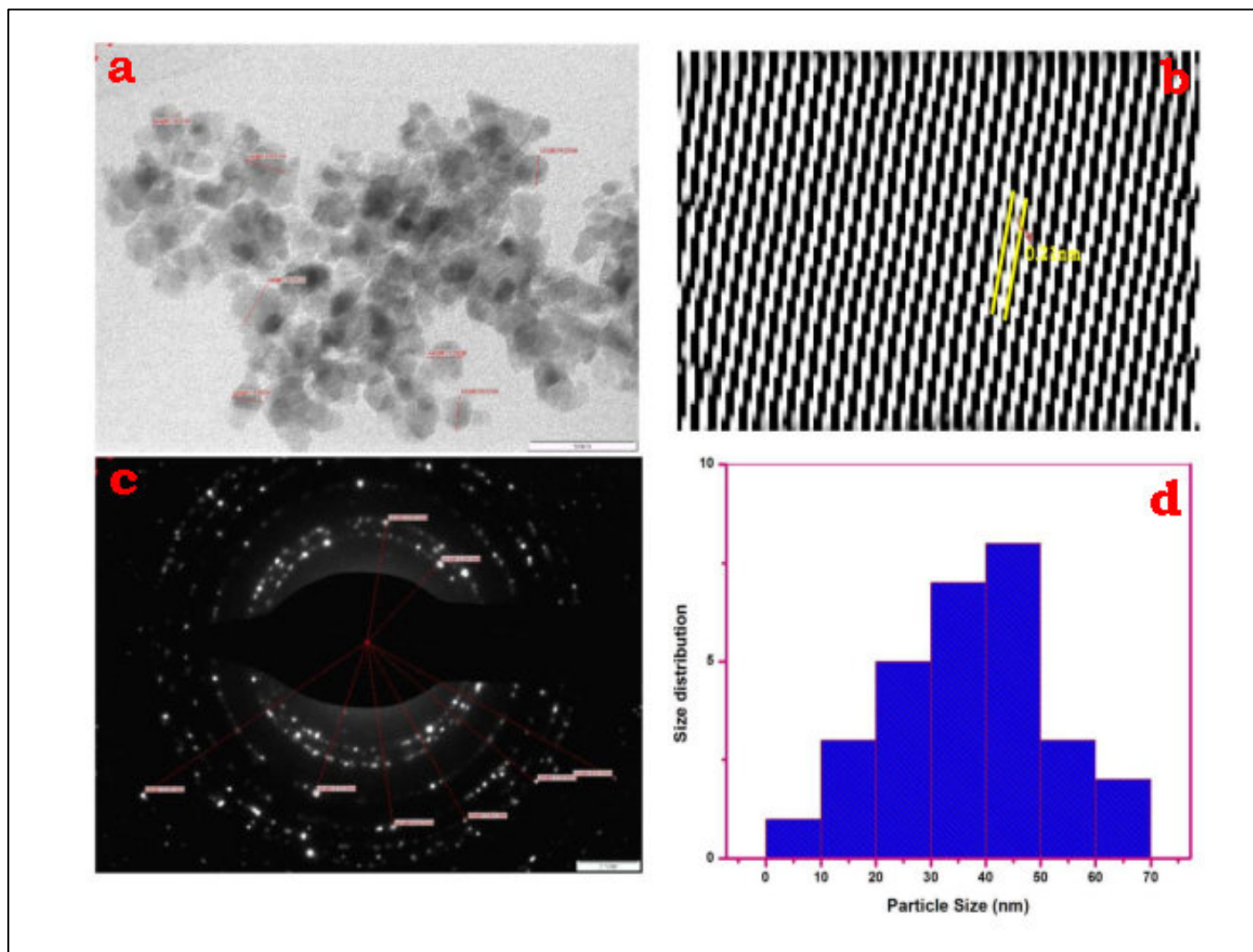


Figure 6: (a) HR-TEM image; (b) lattice fringe; (c) SAED pattern; (d) particle size of biosynthesized CeO₂-NPs

Antioxidant activity of Synthesized nanoparticles by using DPPH method:

DPPH Radical *Trianthema portulastrum* leaf extract scavenging activity Chem CeO₂-Nps and CeO₂-Nps are measured at various concentrations of (25/50/100/125/250/500 μ g /ml) for standard ascorbic acid. By changing DPPH color, from the initial blue/purple solution to a yellow the reduced activity of *Trianthema portulastrum* leaf extract, bioCeO₂-NP, and chemCeO₂-Nps is determined. The percentage of DPPH inhibition is shown in **Figure**

9 & Table 3. For *Trianthema portulastrum* leaf extract, chem CeO₂-Nps bio CeO₂-Nps, and the standard, the calculated half maximum inhibitory concentration (IC₅₀ μ g / ml) values shall be 102.52, 104.86, 95.17 and 88.49. When IC₅₀ μ g / ml values are lower, the potential for extract antioxidant activity is higher. In comparison to *Trianthema portulastrum* leaf and chemical CeO₂-NP, the study of DPPH scavenging activity has seen the greatest inhibition in bio CeO₂-Nps. This result is following Fatemeh et al. studies, which have demonstrated the antioxidant activity of

Ceratonia siliqua extract plants using bio CeO₂-Nps [47]. Moreover, the results of Krishanaveni *et al.* [49] were comparable by the use of *Clitoria ternatea* bio CeO₂-Nps. Antioxidant activities might be related by the presence of flavonoids, alkaloids in the extract of *Trianthema portulastrum* leaf. This means a reduction in antioxidant activity may result in a reduction in the metabolite concentration of

plants during nanoparticulate formation. The surface area of cerium oxide is large, which means more plant chemical substances are added to the active surface. As a result, the shell response phenomenon in the extract of *Trianthema Portulastrum* leaves is elevated by bio CeO₂-Nps (due to an adsorbed antioxidant moiety on the surface).

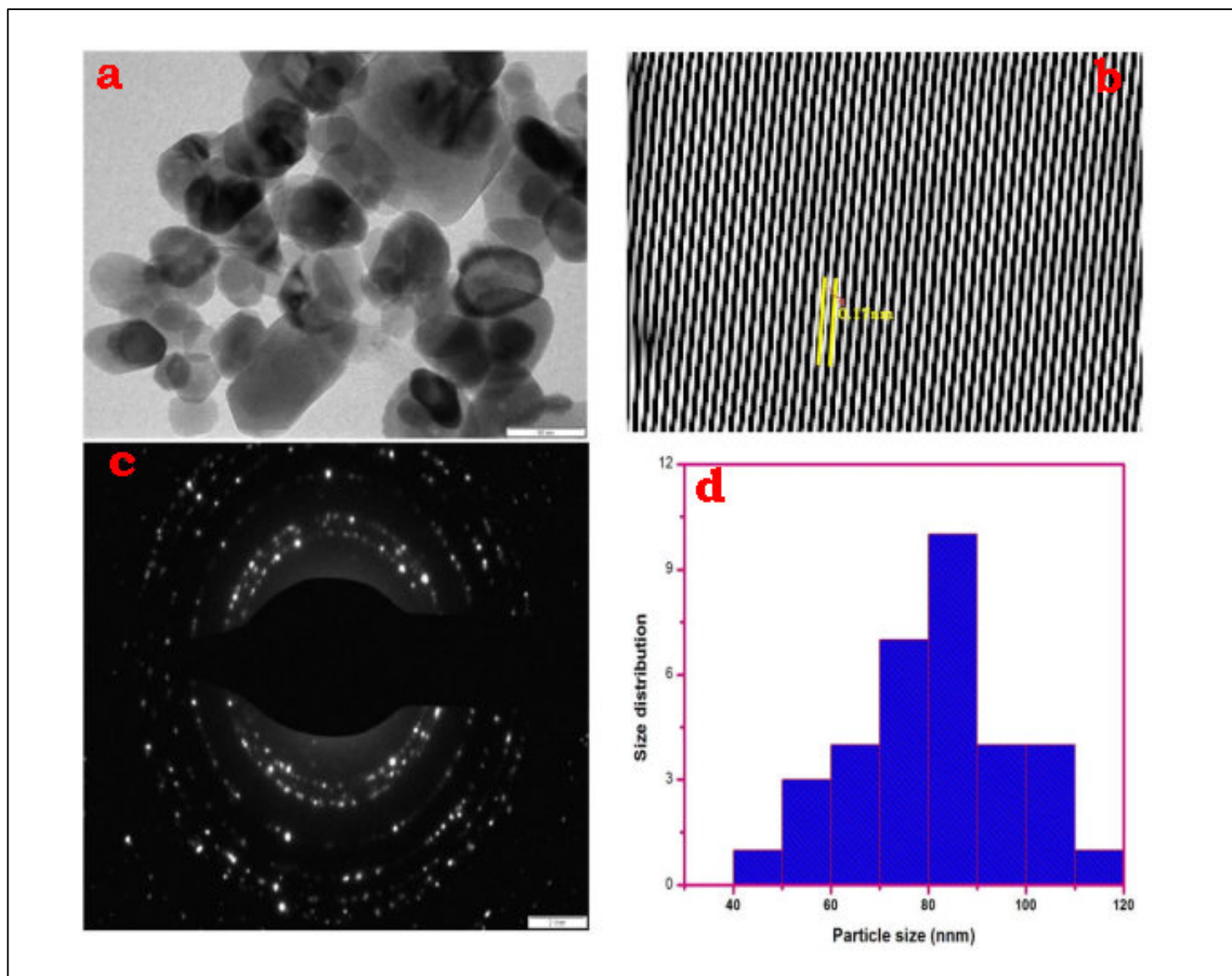


Figure 7: (a) HR-TEM image; (b) lattice fringe; (c) SAED pattern; (d) particle size of Chem CeO₂-NPs

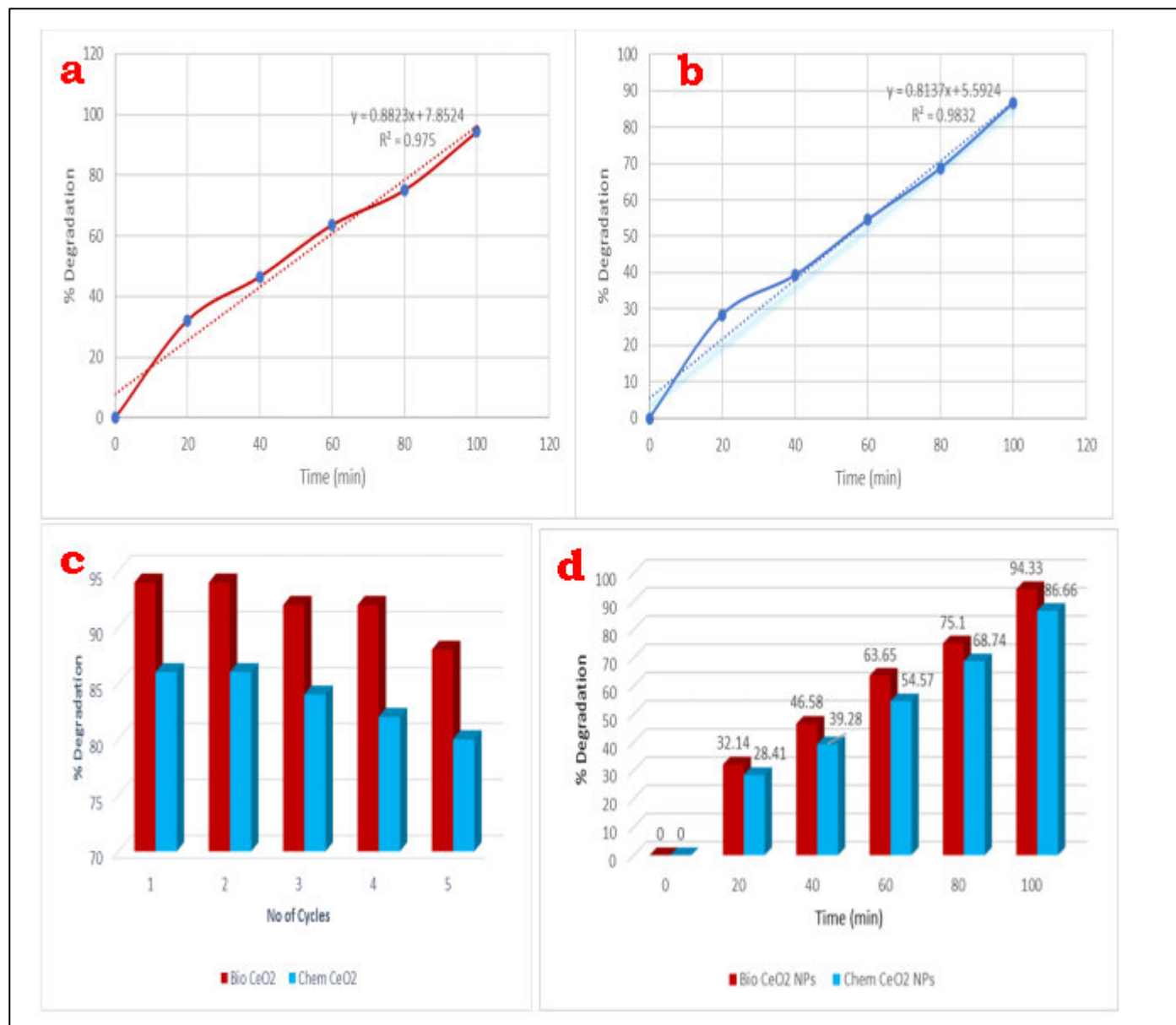


Figure 8: (a & b) Rate constant (K) and regression (R²); (c) Reusability of biosynthesized CeO₂-NPs and Chem CeO₂-NPs; (d) % degradation of acid black 1 dye compared to the biosynthesized CeO₂-NPs and Chem CeO₂-NPs

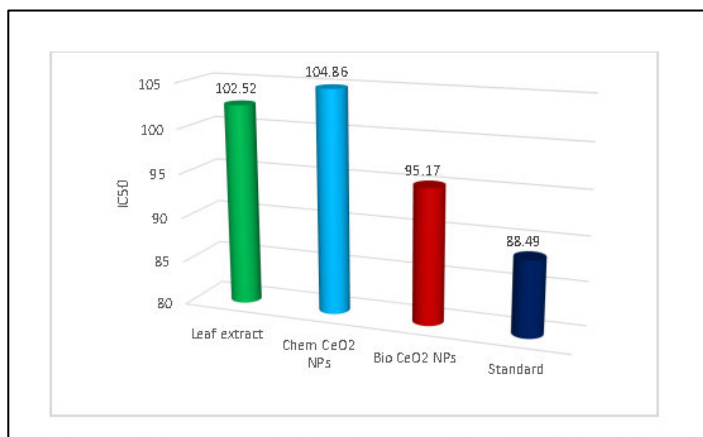


Figure 9: DPPH free radical assay of *Trianthema portulastrum* leaf extract, ChemCeO₂-NPs and biosynthesized CeO₂-NPs

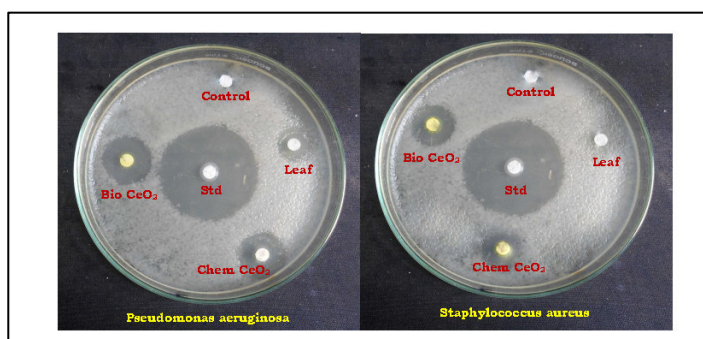


Figure 10: Antibacterial activity of *Trianthema portulastrum* leaf extract, Chem CeO₂-NPs and biosynthesized CeO₂-NPs against *Pseudomonas aeruginosa* and *Staphylococcus aureus*

Table 4: Antibacterial activity of *Trianthema Portulastrum* leaf extract, Chem CeO₂-NPs and biosynthesized CeO₂-NPs against *Pseudomonas aeruginosa* and *Staphylococcus aureus* at 100µL

| Compound | Zone of Inhibition (mm) | |
|---------------------------|--|---------------------------------------|
| | <i>Pseudomonas aeruginosa</i> 100µl | <i>Staphylococcus aureus</i> 100µl |
| Leaf extract | 10±0.08 | 06±0.41 |
| Chem CeO ₂ NPs | 14±0.23 | 11±0.57 |
| Bio CeO ₂ NPs | 17±0.56 | 16±0.24 |
| Standard | 26±0.89 | 26±0.11 |

Antibacterial activity by using disc diffusion method:

Bacterial inhibition of *Trianthema portulastrum* extract, ChemceO₂-NP and bio CeO₂-Nps are analyzed and the area of inhibition is measured for Gram-positive Bacteria (*Staphylococcus aureus*) and

Grass negative Bacteria (*Pseudomonas aeruginosa*) at 100 µl (Figure 10). Table 4 shows the diameter of the inhibition zone (mm). The bio CeO₂-Nps (17±0.56 & 16±0.24) exhibit improved bacteriocidal efficiency than Chem CeO₂-Nps (14±0.23 & 11±0.57) and *Trianthema portulastrum* leaf extracts (10±0.08 & 06±0.41) against *Pseudomonas aeruginosa* and *Staphylococcus aureus*. Particle size and surface area are known to play a key role in their connection with biological cells or to produce secondary damaging products. Due to their size and wide surface area, CeO₂-Nps produce electronic effects. These electronic effects improve nanoparticles' coupling quality with the microbes CeO₂-Nps can therefore easily be attached and inserted into the bacteria in the cell membrane [48]. The above mechanisms show that bio CeO₂-Nps have higher antibacterial activity in comparison with the leaf extract of *Trianthema portulastrum* and Chem CeO₂-Nps. The increased inhibitory activity of bio ceO₂-Nps depends not only on the size of nanoparticles and their surface but also on the capping agents (proteins).

Conclusion:

The bio and chemical CeO₂-Nps were synthesized, evaluated, characterized and compared for the photocatalytic degradation of organic pollutants. We show that CeO₂-Nps degrades acid black 1 coloring under sunlight in a photocatalytic system. Photocatalyst bio CeO₂-Nps exhibited excellent photocatalytic degradation under visible light irradiation of 94.33%. We also show that the bio CeO₂-Nps have antibacterial activity. Data show that bio CeO₂-Nps is associated with various biological and medical applications.

Reference:

- [1] Charbgoon F *et al.* *International Journal of Nanomedicine*. 2017 **12**:1401.
- [2] Muthuvel A *et al.* *Research on Chemical Intermediates*. 2020 **46**:2705.
- [3] Shah M *et al.* *Materials*. 2015 **8**:7278
- [4] Ocsoy I *et al.* *Materials Letters*. 2018 **212**:45.
- [5] Qu X *et al.* *Accounts of Chemical Research*. 2012 **46**:834.
- [6] Muhd Julkapli N *et al.* *The Scientific World Journal*. 2014 **2014**:1
- [7] Šuligoj A *et al.* *Catalysts*. 2020 **10**:253.
- [8] Dhalla A *et al.* *Antioxidants*. 2018 **7**:97.
- [9] Thakur *et al.* *Journal of Nanobiotechnology*. 2019 **17**: 12
- [10] David ME *et al.* *Materials*. 2020 **13**:2064.
- [11] HE L *et al.* *Journal of Rare Earths*. 2015 **33**:791.
- [12] Dhand C *et al.* *RSC Advances*. 2015 **5**:105003.

- [13] Dahle J *et al.* *International Journal of Environmental Research and Public Health*. 2015 **12**:1253.
- [14] Hoecke KV *et al.* *American Chemical Society*. 2009 **43**:4537.
- [15] Farias IAP *et al.* *BioMed Research International*. 2018 **2018**:1.
- [16] Chen B-H *et al.* *International Journal of Nanomedicine*. 2014 **55**:15.
- [17] Annu A *et al.* *Nanomaterials and Plant Potential*. 2019 **26**: 1.
- [18] Campos EA *et al.* *Journal of Aerospace Technology and Management*. 2015 **7**:267.
- [19] Wallace R *et al.* *Journal of Materials Science*. 2013 **48**:6393.
- [20] Tan L *et al.* *Journal of Nanomaterials*. 2011 **2011**:1.
- [21] Pudovkin MS *et al.* *Journal of Nanotechnology*. 2018 **2018**:1.
- [22] Chowdhury A *et al.* *International Nano Letters*. 2017 **7**:91.
- [23] Chowdhury R *et al.* *RSC Advances*. 2020 **10**:14374.
- [24] Arumugam A *et al.* *Materials Science and Engineering*. 2015 **49**:408.
- [25] Venkatesh KS *et al.* *RSC Advances*. 2016 **6**:42720.
- [26] Mohagheghzadeh A *et al.* *Pharmacognosy Reviews*. 2013 **7**:17.
- [27] Nyoka M *et al.* *Nanomaterials*. 2020 **10**:242.
- [28] Balaji S *et al.* *Bioengineering*. 2020 **7**:26.
- [29] Lingaraju K *et al.* *Acta Metallurgica Sinica*. 2015 **28**:1134.
- [30] Das AJ *et al.* *International Journal of Food Properties*. 2015 **19**:636.
- [31] Qais FA *et al.* *Bioinorganic Chemistry and Applications*. 2019 **2019**:1
- [32] Maqbool Q *et al.* *International Journal of Nanomedicine*. 2016 **11**:5015.
- [33] Kundu S *et al.* *Journal of Nanoparticle Research*. 2012 **14**:8
- [34] Edvinsson T. *Royal Society Open Science*. 2018 **5**:180387.
- [35] Pujar MS *et al.* *Bulletin of Materials Science*. 2019 **43**: 1
- [36] Elemike EE *et al.* *Bulletin of Materials Science*. 2017 **40**:129.
- [37] Gipson K *et al.* *Journal of Spectroscopy*. 2015 **2015**:1.
- [38] Zhuang J *et al.* *Applied Sciences*. 2020 **10**:4345.
- [39] Liu J *et al.* *The Journal of Physical Chemistry C*. 2008 **112**:17127.
- [40] Choe JY. *Materials Research Innovations*. 2002 **6**:238.
- [41] Kernazhitsky L *et al.* *Ukrainian Journal of Physics*. 2016 **61**:482.
- [42] Stetefeld J *et al.* *Biophysical Reviews*. 2016 **8**:409
- [43] Thanh NTK *et al.* *Chemical Reviews*. 2014 **114**:7610
- [44] Toledano M *et al.* *RSC Advances*. 2016 **6**:45265.
- [45] Hezam A *et al.* *ACS Applied Nano Materials*. 2019 **3**:138.
- [46] Jawad AH *et al.* *Journal of Taibah University for Science*. 2016 **10**:352.
- [47] Kähkönen MP *et al.* *Journal of Agricultural and Food Chemistry*. 1999 **47**:3954.
- [48] Feng Q *et al.* *International Journal of Environmental Research and Public Health*. 2019 **16**:4029.

Edited by P Kanguane

Citation: Swetharanyam & Kunjitham, *Bioinformation* 16(10): 765-778 (2020)

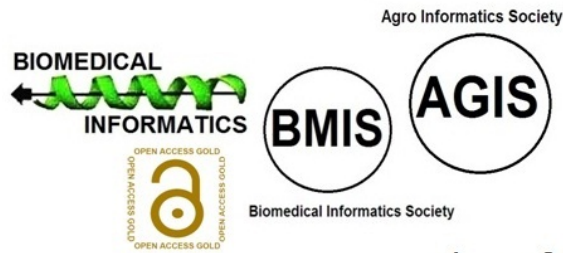
License statement: This is an Open Access article which permits unrestricted use, distribution, and reproduction in any medium, provided the original work is properly credited. This is distributed under the terms of the Creative Commons Attribution License



Articles published in BIOINFORMATION are open for relevant post publication comments and criticisms, which will be published immediately linking to the original article for FREE of cost without open access charges. Comments should be concise, coherent and critical in less than 1000 words.

BIOINFORMATION

Discovery at the interface of physical and biological sciences



since 2005

BIOINFORMATION

Discovery at the interface of physical and biological sciences

indexed in

